

MÄRZKE-WHEELER COORDINATES FOR ACCELERATED OBSERVERS IN SPECIAL RELATIVITY

M. PAURI¹ AND M. VALLISNERI²

ABSTRACT. In special relativity, the definition of coordinate systems adapted to generic accelerated observers is a long-standing problem, which has found unequivocal solutions only for the simplest motions. We show that the *Märzke-Wheeler construction*, an extension of the Einstein synchronization convention, produces accelerated systems of coordinates with desirable properties: (a) they reduce to Lorentz coordinates in a neighborhood of the observers' world-lines; (b) they index *continuously* and *completely* the *causal envelope* of the world-line (that is, the intersection of its causal past and its causal future: for well-behaved world-lines, the entire space-time). In particular, Märzke-Wheeler coordinates provide a smooth and consistent foliation of the causal envelope of any accelerated observer into space-like surfaces.

We compare the Märzke-Wheeler procedure with other definitions of accelerated coordinates; we examine it in the special case of stationary motions, and we provide explicit coordinate transformations for uniformly accelerated and uniformly rotating observers. Finally, we employ the notion of *Märzke-Wheeler simultaneity* to clarify the relativistic paradox of the twins, by pinpointing the local origin of differential aging.

1. INTRODUCTION

In the usual textbook special relativity, the distinction between “inertial observer” and “Lorentz coordinate frame” is blurred. Because of the symmetries of Minkowski space-time, inertial observers can label all the events of space-time in a simple and consistent manner that is based on physical conventions and idealized procedures. (For example, inertial observers can be thought to set up Lorentz coordinate frames via a framework of ideal clocks and rigid rods that extend throughout the space-time region of interest, outfitting it with suitable measuring devices; the clocks are synchronized with light signals; and so on. See, for instance, [1].)

For inertial observers, Lorentz coordinates are a device to extend their concept of physical reality from their world-line to the entire space-time, building a description of the world which incorporates notions of *distance*, and *simultaneity*. What is more, this description of physics is translated easily between inertial observers in relative motion with respect to each other, by the transformations of the Poincaré group.

Date: June 28, 2000.

¹Dipartimento di Fisica, Università di Parma, 43100 Parma, Italy; INFN, Sezione di Milano, Gruppo Collegato di Parma, Italy. E-mail address: pauri@parma.infn.it

²Theoretical Astrophysics 130-33, Caltech, Pasadena CA 91125; Dipartimento di Fisica, Università di Parma, 43100 Parma, Italy; INFN, Sezione di Milano, Gruppo Collegato di Parma, Italy. E-mail address: vallis@tapir.caltech.edu

It follows that in special relativity many physical notions have a joint local and global valence: they are defined with reference to the *entire* Minkowski space-time, but they also carry a well-defined meaning for *local* inertial observers. An instance is the notion of “particle” in quantum field theory (see, e. g., [2, 3]), which corresponds to a *global*, quantized classical mode of the field extending across Minkowski space-time, but also to the outcome of *local* detections along an observer’s trajectory.

Now, suppose we are interested in the observations made by *non-inertial* observers: of course we could study their physics in some given “laboratory” inertial frame of reference. Yet if we could rewrite all equations in a set of coordinates that is somehow *adapted and natural* to the observers’ accelerated motion, we would obtain an interesting representation of the “intrinsic” physics that the accelerated observers experience and theorize about. A well-known example is the Unruh effect [4], where “laboratory” physics predicts that a uniformly accelerated observer moving through the Minkowski quantum vacuum will behave as if in contact with a thermal bath, while “intrinsic” physics describes the Minkowski vacuum as consisting of a thermal distribution of quantum “particles”, as defined by the accelerated observer.

2. DEFINITION OF COORDINATES FOR ACCELERATED OBSERVERS

We set out to define an adapted coordinate system for an accelerated observer (we shall call him “Axel”) who is moving through Minkowski space-time. Since the accelerated system should describe Axel’s “intrinsic” physics, its time coordinate should coincide with Axel’s proper time. Moreover, around any event of Axel’s world-line, there is a small neighborhood where the accelerated coordinates should approximate the local, instantaneous Lorentz rest frame. To satisfy these requirements, we can propagate a *Fermi-Walker transported tetrad*³ along Axel’s world-line, and use the tetrad vectors (one of which will point along Axel’s four-velocity) to reach out to Axel’s surroundings.

How do we extend these prescriptions to cover the entire Minkowski space-time? We can define *extended-tetrad coordinates* by stretching out rigidly the Fermi-Walker transported axes beyond Axel’s immediate vicinity, but we run into trouble soon: for instance, if Axel (a) starts at rest, (b) moves for a while with constant acceleration $|a| = g$, then (c) continues with constant velocity (see Fig. 1), we find that the constant-time surfaces of phase (a) overlap with those of phase (c), at a distance of order g^{-1} from Axel’s world-line. The constant-time planes intersect because they are orthogonal to Axel’s four-velocity u^μ , which tilts during accelerated motion.

³ Fermi-Walker transported vectors “change from instant to instant by precisely that amount implied by the change of the four-velocity” [1]; the transported four-vectors for Axel then obey

$$(1) \quad \frac{dv^\mu}{d\tau} = (u^\mu a^\nu - u^\nu a^\mu) v_\nu,$$

where τ is Axel’s proper time, $u^\mu = dx^\mu/d\tau$ his four-velocity, and $a^\mu = du^\mu/d\tau$ his acceleration.

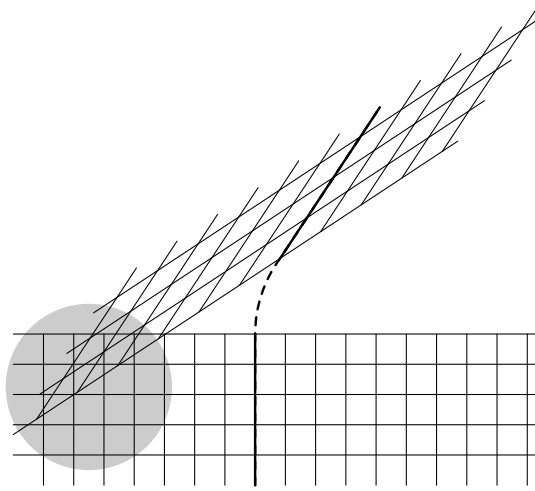


FIGURE 1: World-line of an observer who undergoes a brief period of acceleration (shown dashed). Extension of the *Fermi-Walker transported* coordinate system runs into trouble when different constant-time surfaces overlap on the left. (Adapted from [1].)

3. THE MÄRZKE-WHEELER PROCEDURE

We need a way to *foliate* Minkowski space-time into *non-overlapping surfaces of simultaneity* that are adapted to Axel's motion and that reduce to local Lorentz frames around his world-line. Märzke and Wheeler [5] discussed an extension of *Einstein's synchronization convention*⁴ to synchronize observers in curved space-time. The notion of Märzke-Wheeler simultaneity, *restricted to accelerated observers in flat space-time*, has just the properties we need⁵. We use it to build *Märzke-Wheeler coordinates*, specified as follows. Imagine that: (a) at each event along his world-line $\mathcal{P}(\tau)$, accelerated observer Axel emits a flash of light imprinted with his proper time; (b) in the spatial region that Axel wants to monitor, there are labeling devices capable of receiving Axel's flashes and of sending them back with their signature; (c) Axel is always on the lookout for returning signals (see Fig. 2a). Now, suppose that at event \mathcal{Q} a labeling device receives and rebroadcasts a light flash originally emitted by Axel at proper time τ_1 , and that Axel receives the returning signal at proper time τ_2 . Then Axel will *conventionally* label \mathcal{Q} with a time coordinate $\bar{\tau} = (\tau_1 + \tau_2)/2$ and a radial coordinate $\sigma = (\tau_2 - \tau_1)/2$. These two coordinates can then be completed by two angular coordinates which specify the direction of \mathcal{Q} with respect to $\mathcal{P}(\bar{\tau})$.

If $\mathcal{P}(\tau)$ is an inertial world-line, the constant- $\bar{\tau}$ surfaces are just constant Lorentz-time surfaces, and σ is simply the radius of \mathcal{Q} in spherical Lorentz coordinates (see Fig. 2b): for inertial observers, Märzke-Wheeler coordinates reduce to Lorentz coordinates (see App. C for a proof in a special case). Even

⁴By Einstein's convention, the one-way speed of light between two inertial world-lines is taken to be equal to the average round-trip speed.

⁵Our construction bears resemblance to some applications of Milne's *k-calculus* [6] and to other arguments in the literature [7, 8, 9].

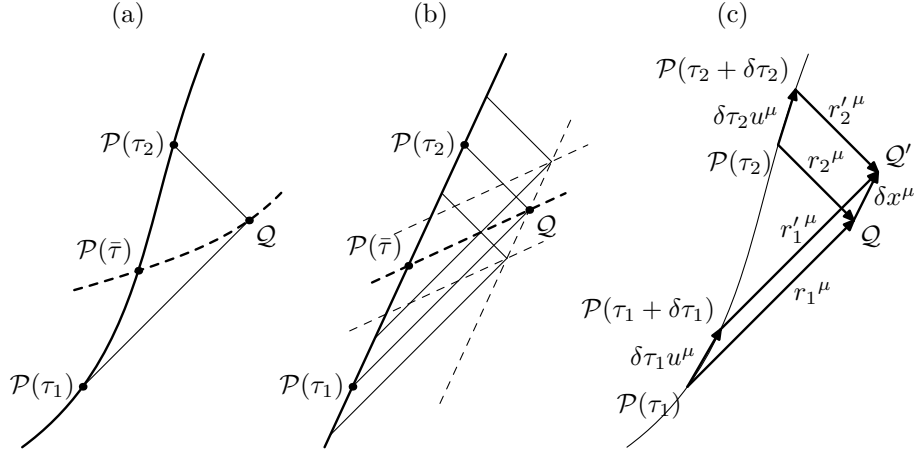


FIGURE 2: Definition of Märzke-Wheeler coordinates. (a): General case. (b): Inertial case. Märzke-Wheeler coordinates reproduce a Lorentz frame. (c): Proof that the constant- $\bar{\tau}$ surfaces are space-like (see p. 4).

better, this procedure yields well-defined coordinates $\bar{\tau}$ and σ for any event Q that lies in the intersection of the causal past and causal future⁶ of the world-line $\mathcal{P}(\tau)$ (we shall refer to this set as the *causal envelope* of $\mathcal{P}(\tau)$; it contains all the events from which bi-directional communication with Axel is possible). Proof: (a) the past and future light-cones of Q necessarily intersect with $\mathcal{P}(\tau)$ somewhere, by definition of causal future and past; (b) the intersection of a null surface with a time-like curve is unique, so once Q is given, τ_1 and τ_2 are well-defined. It follows also that constant- $\bar{\tau}$ surfaces cannot intersect.

We shall use the notation $\Sigma_{\bar{\tau}}$ to refer to the surface of simultaneity labeled by the Märzke-Wheeler time $\bar{\tau}$. To prove that each $\Sigma_{\bar{\tau}}$ is space-like, refer to Fig. 2c, and consider a point Q' that is displaced infinitesimally from Q ; the future light cone with origin in Q' intersects Axel's world-line at the event $\mathcal{P}(\tau_2 + \delta\tau_2)$. Define

$$\begin{aligned}
 r_2^\mu &\equiv (Q - \mathcal{P}(\tau_2))^\mu, \\
 r_2'^\mu &\equiv (Q' - \mathcal{P}(\tau_2 + \delta\tau_2))^\mu, \\
 \delta x^\mu &\equiv (Q' - Q)^\mu;
 \end{aligned}
 \tag{2}$$

both r_2^μ and $r_2'^\mu$ are null vectors. Since the displacements are infinitesimal, we can write

$$(\mathcal{P}(\tau_2 + \delta\tau_2) - \mathcal{P}(\tau_2))^\mu = \delta\tau_2 u^\mu(\tau_2)
 \tag{3}$$

⁶See Wald [10], ch. 8, for these and other definitions concerning the causal structure of space-time.

(u^μ is Axel's four-velocity). Then we have

$$\begin{aligned}
 0 &= |r_2'^\mu|^2 = |r_2^\mu + \delta x^\mu - \delta \tau_2 u^\mu|^2 = \\
 (4) \quad &= |r_2^\mu|^2 + 2 r_2^\mu (\delta x_\mu - \delta \tau_2 u_\mu) + O(\delta \tau^2) = \\
 &= 2 r_2^\mu (\delta x_\mu - \delta \tau_2 u_\mu) + O(\delta \tau^2),
 \end{aligned}$$

and

$$(5) \quad \frac{\partial \tau_2}{\partial x^\mu} = \frac{r_{2\mu}}{r_2^\nu u_\nu(\tau_2)}.$$

The same relation holds for $\partial \tau_1 / \partial x^\mu$:

$$(6) \quad \frac{\partial \tau_1}{\partial x^\mu} = \frac{r_{1\mu}}{r_1^\nu u_\nu(\tau_1)},$$

where $r_1^\mu \equiv (\mathcal{Q} - \mathcal{P}(\tau_1))^\mu$. So we can write the normal vector to the constant- $\bar{\tau}$ surface as

$$(7) \quad \frac{\partial \bar{\tau}}{\partial x^\mu} = \frac{1}{2} \left(\frac{\partial \tau_1}{\partial x^\mu} + \frac{\partial \tau_2}{\partial x^\mu} \right) = \frac{1}{2} \left(\frac{r_{1\mu}}{r_1^\nu u_\nu(\tau_1)} + \frac{r_{2\mu}}{r_2^\nu u_\nu(\tau_2)} \right).$$

Furthermore,

$$(8) \quad \left| \frac{\partial \bar{\tau}}{\partial x^\mu} \right|^2 = \frac{r_1^\mu r_{2\mu}}{(r_1^\nu u_\nu(\tau_1)) (r_2^\nu u_\nu(\tau_2))}.$$

Looking at Fig. 2c, you can convince yourself that $r_1^\mu r_{2\mu} > 0$, $r_1^\nu u_\nu(\tau_1) > 0$, and $r_2^\nu u_\nu(\tau_2) < 0$ (throughout the paper we set $c = 1$ and take a time-like metric). Consequently, the surfaces of constant- $\bar{\tau}$ have normal vectors that are time-like everywhere. Under appropriate hypotheses of smoothness for the world-line $\mathcal{P}(\tau)$, the constant- $\bar{\tau}$ surfaces will also be differentiable; altogether, they qualify as space-like.

Whereas the constant-time surfaces obtained by the extended-tetrad procedure (described in Sec. 2) are always three-dimensional planes, *the global shape of the Märzke-Wheeler constant- $\bar{\tau}$ surfaces depends on the entire history of the observer, both past and future*. Accordingly, the three-dimensional metric ${}^3g_{ij}$ induced by the Minkowski metric on the surfaces will depend on $\bar{\tau}$. This is true in general, but not for *stationary world-lines*, defined by

$$(9) \quad \forall \tau, |\mathcal{P}(\tau + \Delta\tau) - \mathcal{P}(\tau)| = |\mathcal{P}(\tau) - \mathcal{P}(0)|,$$

Stationary world-lines represent motions that show the same behavior at all proper times; in this case, the surfaces $\Sigma_{\bar{\tau}}$ always maintain the same shape and metric. Synge [11] and Letaw [12] obtained stationary world-lines by the alternative definition of relativistic trajectories with constant acceleration and curvatures. In App. A, we briefly review their classification, as given by Synge [11].

You can easily build a stationary trajectory by taking any time-like integral curve of the isometries of Minkowski space-time, and rescaling its parametrization to obtain a world-line that satisfies $u^\mu u_\mu = -1$. Indeed, in this way we can obtain *any* stationary trajectory, because we can always write its four-velocity as a linear combination U^μ of the ten Minkowski Killing fields⁷ (i. e., the infinitesimal generators of isometries). The simplest

⁷They are the four translations $\partial_t, \partial_x, \partial_y, \partial_z$, the three boosts $x \partial_t + t \partial_x, y \partial_t + t \partial_y, z \partial_t + t \partial_z$, and the three rotations, $y \partial_z - z \partial_y, z \partial_x - x \partial_z, x \partial_y - y \partial_x$.

case of stationary trajectories are inertial world-lines, obtained by combining the Killing fields of a time translation and a space translation; further examples are linear uniform acceleration and uniform rotation, obtained as the integral curves of, respectively, a Lorentz boost and a rotation plus time translation.

No matter how we choose to define the constant-time surfaces of a stationary observer (call her “Stacy”), the Killing field U^μ (which coincides with u^μ on Stacy’s world-line, but is defined all over Minkowski space-time) generates infinitesimal translations in time that carry each constant-time surface into the next one, while conserving its three-metric. Once Stacy has chosen a *single* constant-time surface and a set of spatial coordinates to describe it, she can use U^μ to propagate the surface and its coordinates forward and backward in time, defining coordinates for the entire Minkowski space-time.

4. MÄRZKE-WHEELER COORDINATES FOR STATIONARY OBSERVERS: EXAMPLES

Stationary curves are a very useful arena to compare Märzke-Wheeler coordinates with other accelerated systems, such as the stationary coordinates derived by Letaw and Pfautsch [13]. As a first example, suppose Stacy moves with linear, uniform acceleration in (1+1)-dimensional Minkowski space-time⁸. We can write the trajectory as

$$(10) \quad \begin{cases} t = g^{-1} \sinh g\tau, \\ x = g^{-1} \cosh g\tau, \end{cases} \quad (\textit{Hyper-Stacy: world-line})$$

which is an integral curve of the infinitesimal Lorentz boost $U^\mu = g(x\partial_t + t\partial_x)$, where g is the magnitude of the acceleration. In this case, the extended-tetrad procedure gives the traditional Rindler coordinates [14]:

$$(11) \quad \begin{cases} t = g^{-1}(1 + \xi) \sinh g\tau, \\ x = g^{-1}(1 + \xi) \cosh g\tau. \end{cases} \quad (\textit{Hyper-Stacy: Rindler coordinates})$$

You can check easily that the flow of U^μ carries the constant- τ surfaces backward and forward in τ , and that the *Rindler metric* $ds^2 = -(1+g\xi)^2 d\tau^2 + d\xi^2$ is always conserved. Let us now derive Märzke-Wheeler coordinates for Hyper-Stacy’s motion. According to our prescriptions, the surface $\Sigma_{\bar{\tau}=0}$ [the set of the events that are simultaneous to $\mathcal{P}(0)$] includes all the events that, for some σ , receive light signals from $\mathcal{P}(-\sigma)$ and send them back to $\mathcal{P}(\sigma)$. By symmetry, $\Sigma_{\bar{\tau}=0}$ must coincide with the positive- x semiaxis; we then find that the Märzke-Wheeler radial coordinate is $\sigma = g^{-1} \log gx$. Using the finite isometry generated by U^μ with parameter $\bar{\tau}'$, we can now turn $\Sigma_{\bar{\tau}=0}$ into any other $\Sigma_{\bar{\tau}'}$. Altogether, the coordinate transformation between Minkowski and Märzke-Wheeler coordinates is

$$(12) \quad \begin{cases} t = g^{-1} e^{g\sigma} \sinh g\bar{\tau}, \\ x = g^{-1} e^{g\sigma} \cosh g\bar{\tau}. \end{cases} \quad (\textit{Hyper-Stacy: M.-W. coordinates})$$

The Rindler and Märzke-Wheeler constant-time surfaces coincide, and indeed the two coordinate sets are very similar. (If we identify ξ with σ , and τ

⁸Also known as *hyperbolic motion*; in Synge’s classification [11], a *type IIa helix*.

with $\bar{\tau}$, they coincide up to linear order, because both systems must coincide with local Lorentz frames in the vicinity of the world-line).

We turn now to a more interesting example, where Märzke-Wheeler coordinates diverge from conventional wisdom: uniform relativistic rotation⁹. A typical trajectory in 2+1 dimensions for “Roto-Stacy” is

$$(13) \quad \begin{cases} t = \sqrt{1 + R^2 \Omega^2} \tau, \\ r = R, \\ \phi = \Omega \tau, \end{cases} \quad (\text{Roto-Stacy: world-line})$$

where the constant R is the geometric radius of the trajectory, and Ω is the proper angular velocity; the coordinate angular velocity is $d\phi/dt = \Omega/\sqrt{1 + \Omega^2 R^2}$. Finally, Roto-Stacy’s generating Killing vector field is $U^\mu = \sqrt{1 + R^2 \Omega^2} \partial_t + \Omega \partial_\phi$. The traditional coordinate system for Roto-Stacy are rigidly rotating coordinates:

$$(14) \quad \begin{cases} t = \sqrt{1 + R^2 \Omega^2} \tau, \\ r = r', \\ \phi = \phi' + \Omega \tau \end{cases} \quad (\text{Roto-Stacy: rigidly rotating coordinates})$$

(some authors even define $t = \tau$, violating the first requirement we set in Sec. 2). In these coordinates, Roto-Stacy stands fixed in space at $r' = R$, $\phi' = 0$; the constant- τ surfaces coincide with constant- t planes; and the points with fixed r' and ϕ' rotate in the inertial frame with angular velocity $d\phi/dt = \Omega/\sqrt{1 + \Omega^2 R^2}$, which is faster than light for $r' > r'_{\text{lim}} = \sqrt{1 + \Omega^2 R^2}/\Omega$. The metric is

$$(15) \quad \begin{aligned} ds^2 &= - (1 + \Omega^2 R^2) d\tau^2 + r'^2 (d\phi' + \Omega d\tau)^2 + dr'^2 = \\ &= - [1 + (R^2 - r'^2) \Omega^2] d\tau^2 + 2 \Omega r'^2 d\tau d\phi' + r'^2 d\phi'^2 + dr'^2 \end{aligned} \quad (\text{Roto-Stacy: rigidly rotating metric})$$

Now move on to Märzke-Wheeler coordinates, and consider first the surface $\Sigma_{\bar{\tau}=0}$. Märzke-Wheeler coordinates have their origin at Roto-Stacy’s position, $\mathcal{P}(0)$: ($x = R$, $y = 0$). We find the curves of constant σ as the intersection (an ellipse) of the future light cone of $\mathcal{P}(-\sigma)$ with the past light cone of $\mathcal{P}(\sigma)$. As σ increases, the ellipses move outward, weaving the surface $\Sigma_{\bar{\tau}=0}$, which turns out to be defined by (see App. B):

$$(16) \quad \begin{cases} t = c(\sigma) \sin \theta, \\ x = b(\sigma) \cos \theta + R \cos \Omega \sigma, \\ y = a(\sigma) \sin \theta, \end{cases} \quad (\text{Roto-Stacy: M.-W. coord., } \bar{\tau} = 0)$$

where $a(\sigma) = \sqrt{1 + R^2 \Omega^2} \sigma$, $c(\sigma) = R \sin \Omega \sigma$, and $b(\sigma) = \sqrt{a^2(\sigma) - c^2(\sigma)}$ (our choice of the angular coordinate is conventional, but convenient). As σ increases, the centers of the ellipses oscillate on the x -axis between R and $-R$; the semi-axes $a(\sigma)$ and $b(\sigma)$ grow in such a way that no two ellipses ever intersect; and the ellipses themselves pitch up and down in the time

⁹In Synge’s classification [11], a *type IIc helix*.

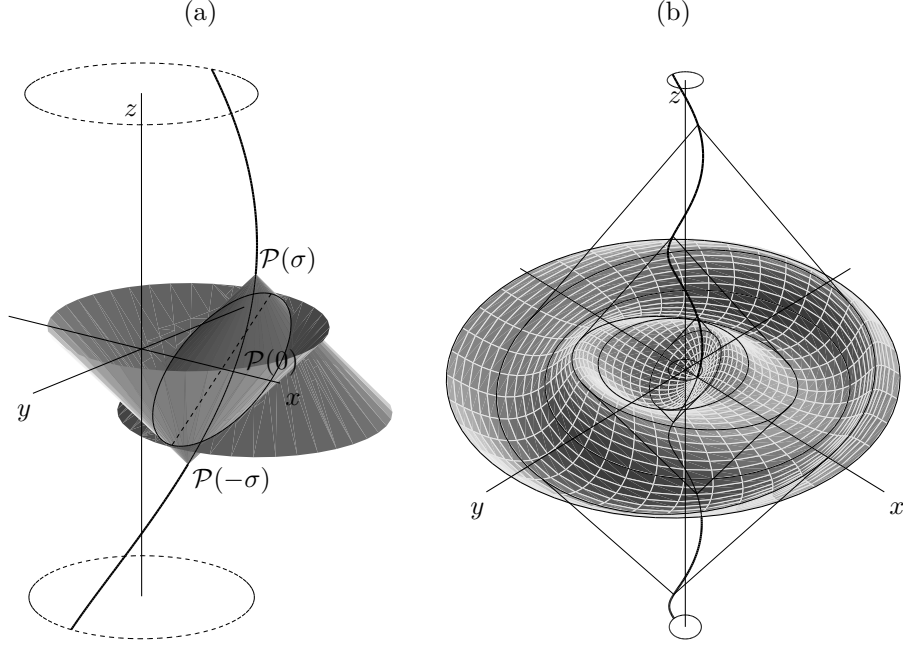


FIGURE 3: Geometry of constant- $\bar{\tau}$ surfaces for uniformly rotating observers. (a): Intersection of the light cones with origin in $\mathcal{P}(-\sigma)$ and $\mathcal{P}(\sigma)$ defines an ellipse. (b) Union of all constant- σ ellipses weaves the constant- $\bar{\tau}$ surface. Notice the oscillating pitch of the ellipses.

direction, as if they were hinging on the y -axis (see Fig. 3), so the Märzke-Wheeler constant- $\bar{\tau}$ surface $\Sigma_{\bar{\tau}=0}$ deviates in undulatory fashion with respect to the Minkowski constant-time surface $t = 0$ [because any event \mathcal{Q} looks closer if the emission and detection events, $\mathcal{P}(-\sigma)$ and $\mathcal{P}(\sigma)$, are on the near side of the origin; it looks farther if they are on the other side]. In the limit $\sigma \rightarrow \infty$, the constant- σ ellipses turn into circles; but the undulation in the t direction maintains the finite amplitude R .

We use the isometry generated by U^μ to propagate these coordinates from $\Sigma_{\bar{\tau}=0}$ throughout Minkowski space-time. The complete transformation between Minkowski and Märzke-Wheeler coordinates is then

$$(17) \quad \begin{cases} t = c(\sigma) \sin \theta + \sqrt{1 + R^2 \Omega^2} \tau, \\ \begin{pmatrix} x \\ y \end{pmatrix} = \begin{pmatrix} \cos \Omega \tau & -\sin \Omega \tau \\ \sin \Omega \tau & \cos \Omega \tau \end{pmatrix} \cdot \begin{pmatrix} b(\sigma) \cos \theta + R \cos \Omega \sigma \\ a(\sigma) \sin \theta \end{pmatrix}. \end{cases}$$

5. MÄRZKE-WHEELER COORDINATES AND THE RELATIVISTIC PARADOX OF THE TWINS

Märzke-Wheeler coordinates cast a new light on the relativistic *paradox of the twins*¹⁰. This *gedankenexperiment* earns the designation of “paradox”

¹⁰The literature on the subject is immense and often redundant. Even if the paradox was already present in Einstein’s 1905 seminal paper [15], it was P. Langevin who first presented it in its modern form. Arzeliès [16] and Marder [17] give excellent annotated bibliographies for contributions up to, respectively, 1966 and 1971.

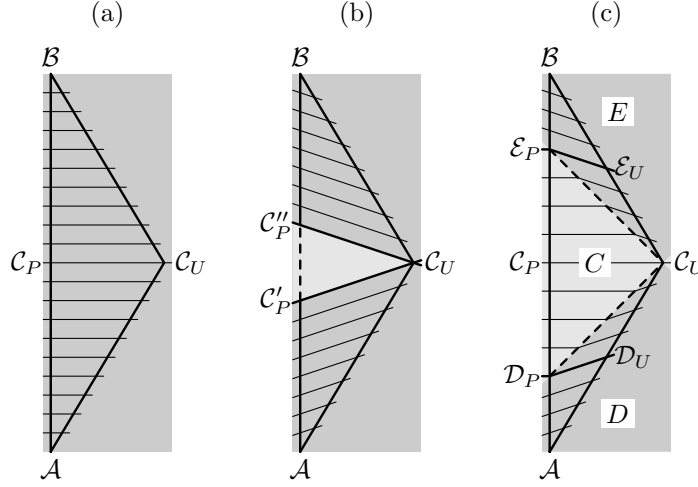


FIGURE 4: The relativistic *paradox of the twins*. The world-lines of the twins are drawn in the Lorentz rest frame of the inertial twin, Penelope, who moves in space-time from \mathcal{A} to \mathcal{B} through \mathcal{C}_P . The journeying twin, Ulysses, travels first from \mathcal{A} to \mathcal{C}_U with velocity v , then inverts his motion to rejoin Penelope in \mathcal{B} . (a): Lorentz slicing of space-time according to Penelope. (b): Lorentz slicing of space-time according to Ulysses, on his separate stretches of inertial motion. Ulysses skips a finite lapse of Penelope's world-line (shown dashed). (c): Märzke-Wheeler slicing of space-time, according to Ulysses. This slicing coincides with the Lorentz slicing in (b) for events in the regions D and E (these events belong to the causal envelopes of the world-line segments $\mathcal{A}\mathcal{C}_U$ and $\mathcal{C}_U\mathcal{B}$), but it shows a peculiar structure in region C .

because, at first sight, the motion of the twins is reciprocal, whereas the physical effects of relativistic time dilation are not. In the usual arrangement, shown in Fig. 4a, the journeying twin (“Ulysses”) moves with constant speed v , first away from and then toward the waiting, inertial (and non-identical!) twin “Penelope”. According to the Lorentz transformation between the inertial frames associated with the twins, Penelope sees Ulysses’ proper time as dilated by the relativistic factor $\gamma = (1 - v^2)^{-1/2} > 1$, so when the twins are rejoined, Penelope has aged γ^{-1} times as much as Ulysses. Yet, it is also true that Penelope always moves with a speed v relatively to Ulysses, so *he* should see *her* proper time as dilated!

The problem is that the notion of time dilation, as it is usually discussed, amounts to little more than a statement on how to relate the coordinate times of different Lorentz frames; it also concerns the observations of different inertial observers, whose proper times coincide with the coordinate times of their Lorentz rest frames. Now, Ulysses is *not* an inertial observer *throughout* his motion, because at event \mathcal{C}_U he turns around and begins his return trip towards Penelope. Along the world-line segments $\mathcal{A}\mathcal{C}_U$ and $\mathcal{C}_U\mathcal{B}$, it is correct to say that Ulysses sees Penelope’s proper time as dilated, in the following sense: if Ulysses compares his proper time with Penelope’s at events which are simultaneous in his Lorentz rest frame, then Penelope appears to be aging at a slower pace. However, when Ulysses inverts his velocity at \mathcal{C}_U (see Fig. 4b), he switches to a new Lorentz frame, and his

constant-time surfaces change their space-time orientation abruptly. Just before arriving in \mathcal{C}_U , Ulysses considers himself simultaneous to the event \mathcal{C}'_P along Penelope's world-line; just after leaving \mathcal{C}_U , according to his new Lorentz frame, Ulysses considers himself simultaneous to \mathcal{C}''_P . However, \mathcal{C}'_P and \mathcal{C}''_P are distinct events, separated by a finite lapse of time! *There is a finite section of Penelope's world-line which Ulysses effectively skips and to which he is never simultaneous.* Because of this missing finite lapse of Penelope's proper time, Ulysses is younger at his final reunion with Penelope, even if throughout the trip he reckoned that Penelope was aging at a slower pace than him¹¹!

From a general-relativistic perspective, there is no paradox from the beginning: Ulysses and Penelope move on different space-time paths between the same two events. The lapse of proper time is a particular functional of the path followed: no wonder that it is different for the two twins! The surprise of non-reciprocal time dilation arises because (a) Ulysses needs to compare *simultaneous* events on his and on Penelope's world-lines to know who is aging faster, so he needs a global notion of simultaneity or, equivalently, a slicing of space-time into space-like, constant-time surfaces; (b) since our Ulysses has a special-relativistic background, he naturally employs the slicing implicit in his two distinct Lorentz rest frames; (c) but that slicing fails to cover a finite region of space-time, where nevertheless Penelope spends part of her time!

Märzke-Wheeler coordinates avoid this problem, since by definition they provide a consistent time slicing of the causal envelope of any observer's world-line: Ulysses and Penelope stay well inside each other's causal envelope, simply because they start together and cannot travel faster than light. For inertial Penelope, Märzke-Wheeler coordinates reproduce a Lorentz rest frame (Fig. 4a). So nothing changes in her account of Ulysses' aging: her proper time lapse Δt_P is γ^{-1} times Ulysses' proper time lapse Δt_U .

Likewise, Märzke-Wheeler coordinates for Ulysses do reproduce a Lorentz frame, but only and separately for the events in the causal envelopes (D and E) of the segments of Ulysses' uninterrupted inertial motion (\mathcal{AC} and \mathcal{CB} ; see Fig. 4c). In the process of Märzke-Wheeler synchronization, the events in D and E communicate with events along the *same* segment. On the contrary, region C contains events that are space-like related to \mathcal{C} , and that receive light signals from \mathcal{AC} and reflect them back to \mathcal{CB} . It is in this region that the non-inertial character of Ulysses' motion becomes manifest. A simple calculation (App. C) yields the slicing structure shown in Fig. 4c: in D and E the slices assume the typical inclination of Lorentz constant-time surfaces, but in C the slices become perpendicular to \mathcal{AB} (Penelope's world-line), because they split the difference between the two opposing inertial motions \mathcal{AC} and \mathcal{CB} .

¹¹Ulysses' "switch" of Lorentz frames in \mathcal{C}_U has generated some controversy, centered on the physical effects of Ulysses' acceleration around \mathcal{C}_U . These effects are irrelevant, as can be seen by the "third twin" argument introduced by Lord Halsbury [18]: in brief, at \mathcal{C}_U Ulysses communicates the reading of his clock to a third twin who was already traveling towards Penelope with velocity v ; thus, the proper time elapsed on the different paths $\mathcal{AC}_U\mathcal{B}$ and $\mathcal{AC}_P\mathcal{B}$ can be compared without any twin ever experiencing acceleration.

	Ulysses' Δt_U in segment	Ulysses' total t_U	Penelope's Δt_P in segment	Penelope's total t_P	$\frac{dt_P}{dt_U}$ in segment
\mathcal{AD}	$\frac{1}{2(1+v)}$	$\frac{1}{2(1+v)}$	$\frac{1}{2} \frac{1-v}{\sqrt{1-v^2}}$	$\frac{1}{2} \frac{1-v}{\sqrt{1-v^2}}$	$\sqrt{1-v^2}$
\mathcal{DC}	$\frac{v}{2(1+v)}$	$\frac{1}{2}$	$\frac{1}{2} \frac{v}{\sqrt{1-v^2}}$	$\frac{1}{2} \frac{1}{\sqrt{1-v^2}}$	$\frac{1+v}{\sqrt{1-v^2}}$
\mathcal{CE}	$\frac{v}{2(1+v)}$	$\frac{1+2v}{2(1+v)}$	$\frac{1}{2} \frac{v}{\sqrt{1-v^2}}$	$\frac{1}{2} \frac{1+v}{\sqrt{1-v^2}}$	$\frac{1+v}{\sqrt{1-v^2}}$
\mathcal{EB}	$\frac{1}{2(1+v)}$	1	$\frac{1}{2} \frac{1-v}{\sqrt{1-v^2}}$	$\frac{1}{\sqrt{1-v^2}}$	$\sqrt{1-v^2}$

TABLE 1: Evolution of Ulysses' and Penelope's proper times along the segments shown in Fig. 4c; all comparisons are made at events that are simultaneous according to Ulysses' Märzke-Wheeler slicing. The last column shows that Ulysses' ages faster than Penelope's along segments \mathcal{AD} and \mathcal{EB} , but not along \mathcal{DC} and \mathcal{CE} . Units are normalized so that Ulysses' total proper time lapse is 1.

If Ulysses employs the Märzke-Wheeler notion of simultaneity to compare his age with Penelope's at simultaneous times, he accounts for the final aging difference as follows. As long as Penelope's trajectory remains within the regions D and E where the Märzke-Wheeler and Lorentz notions of simultaneity coincide, Ulysses ages γ times faster than Penelope, just as a naïve use of relativistic time dilation would imply. However, when Penelope moves through region C (from \mathcal{D}_P to \mathcal{E}_P), she ages $\gamma^{-1}(1-v)^{-1} > 1$ times faster than Ulysses (who moves from \mathcal{D}_U to \mathcal{E}_U). Altogether, when the twins are rejoined in \mathcal{B} , Ulysses is younger by an overall factor of γ . See Table 1 and Fig. 5 for a precise tally of proper times. In App. D we study Ulysses' Märzke-Wheeler interpretation of Penelope's aging in a modified construction where Ulysses moves with constant speed and acceleration on *Roto-Stacy's* circular trajectory. The resulting $t_P[t_U]$ (Fig. 8) is smooth and resembles qualitatively the function shown in Fig. 5.

Keep in mind that the comparison of local relative aging is dependent on how we slice space-time into constant-time surfaces. Alternative slicings will lead Ulysses to *different distributions* of Penelope's total proper time along his world-line. Stautberg Greenwood [19] defines simultaneity by integrating the Doppler-shifted frequency of monochromatic signals exchanged by the twins. Unruh [20] employs the notion of *parallax distance* to extend Ulysses' local definitions of space and time, to the effect that at times he sees Penelope recede in time. Debs and Redhead [21] analyze the class of slicings induced by Reichenbach's *non-standard synchronies* [22], which generalize the Einstein convention by positing different speeds for the light signals in the two directions. However, we believe that Märzke-Wheeler slicing has a simple physical rationale and that it does a good job of locating the non-reciprocal, differential aging in the region of space-time where the non-local effects of Ulysses' turn-around in \mathcal{C} are felt.

6. CONCLUSIONS

We have shown how to use the Märzke-Wheeler construction to build accelerated systems of coordinates that are *adapted to the motion of an arbitrary*

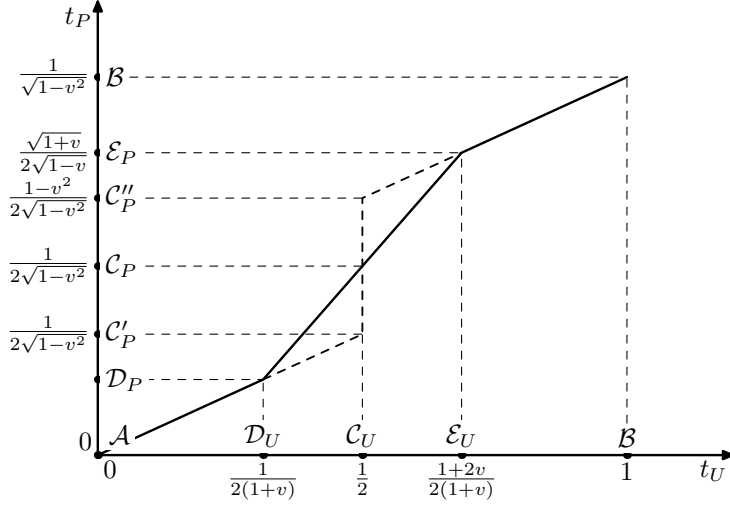


FIGURE 5: Penelope's proper-time, in units of Ulysses' total proper-time lapse, as determined by Ulysses through Lorentz slicing (dashed line, see Fig. 4b) or Märzke-Wheeler slicing (continuous line, see Fig. 4c).

observer in flat space-time, in the sense that: (a) on the observer's world-line, the Märzke-Wheeler time coordinate $\bar{\tau}$ coincides with the observer's proper time τ ; (b) in a neighborhood of the world-line, Märzke-Wheeler coordinates reduce to Lorentz (spherical) coordinates; (c) the procedure assigns smoothly and unambiguously a time $\bar{\tau}$ and a Märzke-Wheeler radial coordinate σ to all events in the *causal envelope* of the world-line (that is, to all events from which bi-directional communication with the observer is possible). This is obtained with a simple geometric construction that generalizes the Einstein synchronization criterion. In particular, we showed that $\bar{\tau}$ indexes a smooth foliation of the causal envelope of the world-line into space-like surfaces.

The Märzke-Wheeler construction is intrinsically global: *the structure of any constant- $\bar{\tau}$ surface depends on the geometry of the entire world-line of the observer*. Yet this global dependence is hierarchical. Take for instance the constant-time surface $\bar{\tau} = \tau_0$, with origin in $\mathcal{P}(\tau_0)$: the behavior of the world-line at proper times that lie to the future of $\tau_0 + \Delta\tau$, or to the past of $\tau_0 - \Delta\tau$, can only influence the structure of the constant-time surface for $\sigma > \Delta\tau$.

We have examined the special case of stationary observers, where Märzke-Wheeler constant-time surfaces are all identical, and they are translated into each other by a family of Minkowski space-time isometries. In the simplest case, hyperbolic motion, Märzke-Wheeler coordinates are related to the familiar Rindler system by a monotonic map between the radial coordinates. In the case of circular motion, however, the Märzke-Wheeler constant- $\bar{\tau}$ surfaces have a much richer structure than the constant-time planes of rigidly rotating coordinates.

Finally, we have discussed how to use the notion of *Märzke-Wheeler simultaneity* to elucidate the relativistic paradox of the twins, by establishing

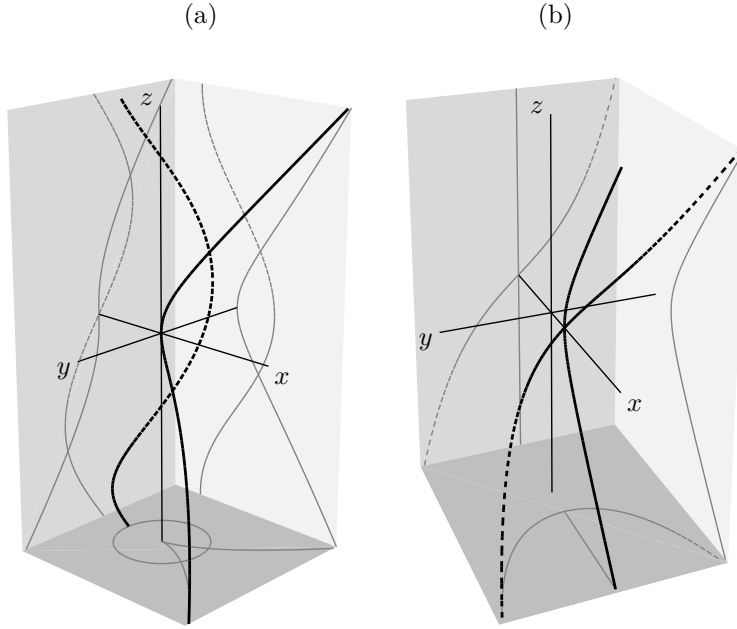


FIGURE 6: Synge's helices. (a): Type IIc (shown dashed), and type IIb helices. (b): Type IIa (dashed), and type III helices. Notice the cusp in the xy -plane projection of the type IIb curve; also notice that the type III helix coincides with projection of the type IIa curve on the xz -plane.

a continuous correspondence between the lapses of proper time experienced by the twins. It is possible to attribute the differential aging of the twins to distinct segments of their world-lines, where we can conclude that one twin is aging faster. Although this attribution is not unique, it is justified physically by recourse to generalized Einstein synchronization, and it is not possible with other definitions of simultaneity (such as a naïve use of instantaneous Lorentz frames).

APPENDIX A. STATIONARY TRAJECTORIES IN FLAT SPACE-TIME (SYNGE'S HELICES)

Synge [11] solved the *relativistic Frenet-Serret equations*,

$$(18) \quad \begin{cases} \dot{u}^\mu = c_1 n_1^\mu, \\ \dot{n}_1^\mu = c_2 n_2^\mu + c_1 u^\mu, \\ \dot{n}_2^\mu = c_3 n_3^\mu - c_2 n_1^\mu, \\ \dot{n}_3^\mu = -c_3 n_2^\mu \end{cases}$$

(where u^μ is the 4-velocity and n_i^μ are the three *normals*), by restricting the curvature coefficients c_1 , c_2 , and c_3 to constants. We briefly summarize Synge's classification of the resulting trajectories (for pedagogical purposes, we invert Synge's enumeration). In Fig. 6, we show examples of these curves.

Inertial world-lines (type IV). All curvatures vanish.

Hyperbolic motion (type III). (*Hyper-Stacy*) $c_2 = c_3 = 0$. The only non-zero curvature is the acceleration. Motion is restricted to a $(1 + 1)$ -dimensional hyperplane; the trajectory is spatially unlimited and the 3-velocity approaches the speed of light asymptotically. In a suitable Lorentz frame, we can write the world-line as

$$(19) \quad \begin{cases} t = c_1^{-1} \sinh c_1 \tau, \\ x = c_1^{-1} \cosh c_1 \tau, \\ y = z = 0, \end{cases} \quad (\text{Type III})$$

where τ is proper time, and c_1 is the magnitude of the acceleration.

Plane helixes (type II). Only $c_3 = 0$: the spatial curvature c_2 allows non-trivial motion in a $(2 + 1)$ -dimensional hyper-plane. There are three subtypes.

Uniform circular motion (Roto-Stacy, type IIc). If $c_2^2 - c_1^2 > 0$, the world-line winds up in a spatially limited domain. It is a circular helix of radius $c_1/(c_2^2 - c_1^2)$ and angular velocity $\sqrt{c_2^2 - c_1^2}$.

$$(20) \quad \begin{cases} t = \frac{c_2}{c_2^2 - c_1^2} \sqrt{c_2^2 - c_1^2} \tau, \\ x = \frac{c_1}{c_2^2 - c_1^2} \cos \sqrt{c_2^2 - c_1^2} \tau, \\ y = \frac{c_1}{c_2^2 - c_1^2} \sin \sqrt{c_2^2 - c_1^2} \tau, \\ z = 0. \end{cases} \quad (\text{Type IIc})$$

Cusped motion (type IIb). If $c_1^2 - c_2^2 = 0$, the result is a run-away curve (although it approaches spatial infinity only cubically in time and not exponentially as type III does), with a peculiar cusp.

$$(21) \quad \begin{cases} t = \tau + \frac{1}{6} c_1^2 \tau^3, \\ x = \frac{1}{2} c_1 \tau^2, \\ y = \frac{1}{6} c_1^2 \tau^3 \\ z = 0. \end{cases} \quad (\text{Type IIb})$$

Skewed hyperbolic motion (type IIa). If $c_1^2 - c_2^2 > 0$, the spatial curvature c_2 is not strong enough to wind up the world-line, which becomes spatially unlimited and approaches asymptotically the speed of light. In fact, this solution may be considered as a type III helix combined with a linear, uniform

motion.

$$(22) \quad \begin{cases} t = \frac{c_1}{c_1^2 - c_2^2} \sinh \sqrt{c_1^2 - c_2^2} \tau, \\ x = \frac{c_1}{c_1^2 - c_2^2} \cosh \sqrt{c_1^2 - c_2^2} \tau, \\ y = \frac{c_2}{c_1^2 - c_2^2} \sqrt{c_1^2 - c_2^2} \tau, \\ z = 0. \end{cases} \quad (\text{Type IIa})$$

General case (type I). All curvatures have a finite value, and the trajectory is truly four-dimensional. The resulting helix is a product (of sorts) between a type III and a type IIc motion, each of which takes place in a 2-dimensional hyperplane.

$$(23) \quad \begin{cases} t = r\chi^{-1} \sinh \chi \tau, \\ x = q\gamma^{-1} \sin \gamma \tau, \\ y = q\gamma^{-1} \cos \gamma \tau, \\ z = r\chi^{-1} \cosh \chi \tau, \end{cases} \quad (\text{Type I})$$

where

$$(24) \quad \begin{cases} \chi^2 = (c_1^2 - c_2^2 - c_3^2 + R)/2, \\ \gamma^2 = (-c_1^2 + c_2^2 + c_3^2 + R)/2, \\ r^2 = [(c_1^2 + c_2^2 + c_3^2)/R + 1]/2, \\ q^2 = [(c_1^2 + c_2^2 + c_3^2)/R - 1]/2, \\ R^2 = (c_1^2 - c_2^2 - c_3^2)^2 + 4c_1^2 c_3^2. \end{cases}$$

APPENDIX B. MÄRZKE-WHEELER COORDINATES FOR UNIFORMLY ROTATING OBSERVERS

Roto-Stacy's world-line is given by (13), and in Cartesian coordinates by

$$(25) \quad \begin{cases} t = \sqrt{1 + R^2 \Omega^2} \tau, \\ x = R \cos \Omega \tau, \\ y = R \sin \Omega \tau. \end{cases} \quad (\text{Roto-Stacy: world-line})$$

We seek equations for the surface $\Sigma_{\bar{r}=0}$, which is generated by the concentric curves $S(\sigma)$ of constant σ : each curve $S(\sigma)$ is defined as the intersection of the future light cone of $\mathcal{P}(-\sigma)$ with the past light cone of $\mathcal{P}(\sigma)$ (see Fig. 7).

A point \mathcal{Q} belongs to the future light cone of $\mathcal{P}(-\sigma)$ if the spatial distance between $\mathcal{P}(-\sigma)$ and \mathcal{Q} equals the coordinate-time difference between them; that is, if

$$(26) \quad |\mathbf{x}[\mathcal{Q}] - \mathbf{x}[\mathcal{P}(-\sigma)]| = t[\mathcal{Q}] - t[\mathcal{P}(-\sigma)] = \Delta t(-\sigma);$$

a similar relation is true for points on the past light cone of $\mathcal{P}(\sigma)$:

$$(27) \quad |\mathbf{x}[\mathcal{Q}] - \mathbf{x}[\mathcal{P}(\sigma)]| = t[\mathcal{P}(\sigma)] - t[\mathcal{Q}] = \Delta t(\sigma).$$

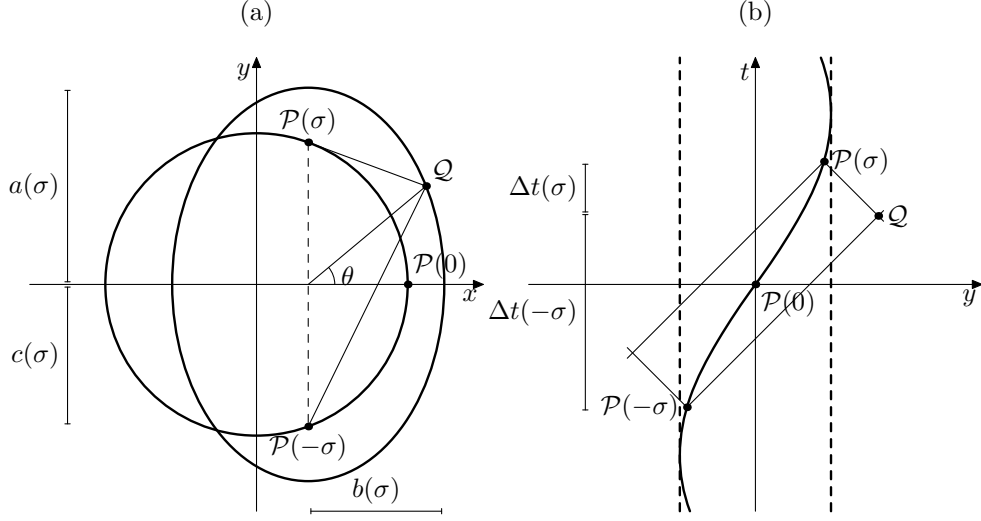


FIGURE 7: Geometric construction of Märzke-Wheeler constant- σ surfaces for *Roto-Stacy*. Her world-line's projection is (a) a circle in the xy plane; (b) a sinusoidal curve in the yt plane (b).

Summing the two equations, we get

$$(28) \quad |\mathbf{x}[\mathcal{Q}] - \mathbf{x}[\mathcal{P}(-\sigma)]| + |\mathbf{x}[\mathcal{Q}] - \mathbf{x}[\mathcal{P}(\sigma)]| = \\ = t[\mathcal{P}(\sigma)] - t[\mathcal{P}(-\sigma)] = \Delta t(\sigma) + \Delta t(-\sigma) = 2\sqrt{1 + R^2\Omega^2}\sigma;$$

that is, the points on $S(\sigma)$ describe an ellipse in the spatial plane. These ellipses have $\mathcal{P}(-\sigma)$ and $\mathcal{P}(\sigma)$ as their foci, and they are centered in $\mathcal{C}(\sigma)$: $(x = R \cos \Omega\sigma, y = 0)$. We parametrize the ellipses in the obvious way,

$$(29) \quad \begin{cases} x = b(\sigma) \cos \theta + R \cos \Omega\sigma, \\ y = a(\sigma) \sin \theta. \end{cases} \quad (\text{ellipses } S(\sigma))$$

The length $a(\sigma)$ of the major semiaxis is given by the half-sum of the distances between any point on $S(\sigma)$ and the two foci:

$$(30) \quad a(\sigma) = \frac{1}{2} \left\{ |\mathbf{x}[\mathcal{Q}] - \mathbf{x}[\mathcal{P}(-\sigma)]| + |\mathbf{x}[\mathcal{Q}] - \mathbf{x}[\mathcal{P}(\sigma)]| \right\} = \sqrt{1 + R^2\Omega^2}\sigma;$$

also, from (25) the half-distance between the foci is $c(\sigma) = R \sin \Omega\sigma$, so we find the length of the minor semiaxis $b(\sigma)$ as

$$(31) \quad b(\sigma) = \sqrt{a^2(\sigma) - c^2(\sigma)} = \sqrt{(1 + R^2\Omega^2)\sigma^2 - R^2 \sin^2 \Omega\sigma}.$$

To complete our characterization of $\Sigma_{\bar{r}=0}$, we need only the coordinate time of the points on the curves $S(\sigma)$. From Fig. 7b we have

$$(32) \quad \begin{aligned} t[\mathcal{Q}] &= t[\mathcal{P}(\sigma)] - \Delta t(\sigma) = \frac{1}{2} \{ \Delta t(-\sigma) + \Delta t(\sigma) \} - \Delta t(\sigma) = \\ &= \frac{1}{2} |\mathbf{x}[\mathcal{Q}] - \mathbf{x}[\mathcal{P}(-\sigma)]| - \frac{1}{2} |\mathbf{x}[\mathcal{Q}] - \mathbf{x}[\mathcal{P}(\sigma)]|; \end{aligned}$$

then by explicit calculation we find that $t[\mathcal{Q}] = c(\sigma) \sin \theta$, using (29)–(31). Altogether we obtain the surface described by (16) and shown in Fig. 3.

Given the symmetry of *Roto-Stacy's* motion, the effect of moving from $\Sigma_{\bar{\tau}=0}$ to $\Sigma_{\bar{\tau}=\Delta\bar{\tau}}$ will be just a translation in t by $\sqrt{1+R^2\Omega^2}\Delta\bar{\tau}$, together with a rotation of x and y by an angle $\Omega\Delta\bar{\tau}$; the complete transformation between Märzke-Wheeler and Lorentz coordinates is therefore that given in (17).

APPENDIX C. MÄRZKE-WHEELER COORDINATES FOR THE PARADOX OF THE TWINS: LINEAR MOTION

For simplicity, we use Penelope's Lorentz coordinates to parametrize Ulysses' world-line (shown in Fig. 4), putting the origin $(0,0)$ in \mathcal{C}_U , so that the world-line is described by $x = -v|t|$. Proceeding as in App. B, we see that the Märzke-Wheeler constant-time surface that is simultaneous to $\mathcal{P}(t_0)$ is given by the events \mathcal{Q} such that, for some s ,

$$(33) \quad \begin{cases} |x[\mathcal{Q}] - x[\mathcal{P}(t_0 - s)]| = t[\mathcal{Q}] - t[\mathcal{P}(t_0 - s)], \\ |x[\mathcal{Q}] - x[\mathcal{P}(t_0 + s)]| = t[\mathcal{P}(t_0 + s)] - t[\mathcal{Q}]. \end{cases}$$

We simplify our notation by setting $t = t[\mathcal{Q}]$ and $x = x[\mathcal{Q}]$, and we insert the explicit form of Ulysses' world-line into (33):

$$(34) \quad \begin{cases} |x + v|t_0 - s| = t - (t_0 - s), \\ |x + v|t_0 + s| = (t_0 + s) - t. \end{cases}$$

If we are concerned only with events to the left of Ulysses' trajectory, the outer absolute values can be exchanged for a minus. Summing and subtracting the equations, we obtain the following expressions for x and t :

$$(35) \quad \begin{cases} -x = s + \frac{1}{2}(v|t_0 - s| + v|t_0 + s|), \\ t = t_0 + \frac{1}{2}(v|t_0 + s| - v|t_0 - s|). \end{cases} \quad (\text{events simultaneous to } \mathcal{P}(t_0))$$

Let us take $t_0 > 0$, and examine Eq. (35): if an event \mathcal{Q} , simultaneous to $\mathcal{P}(t_0)$, belongs to region E of Fig. 4c, both $\mathcal{P}(t_0 - s)$ and $\mathcal{P}(t_0 + s)$ will be in region E . It follows that $t_0 - s > 0$ and $t_0 + s > 0$, and therefore

$$(36) \quad \begin{cases} -x = s + vt_0, \\ t = t_0 + vs. \end{cases} \quad (\text{region } E)$$

In a neighborhood of his world-line, these equations reproduce the slices of his constant Lorentz time. On the other hand, if \mathcal{Q} belongs to region C , then $t_0 - s < 0$, $t_0 + s > 0$, and

$$(37) \quad \begin{cases} -x = (1 + v)s, \\ t = (1 + v)t_0. \end{cases} \quad (\text{region } C)$$

These relations create the flat structure of Märzke-Wheeler slices shown in Fig. 4c. The two coordinate patches of Eqs. (36), (37) join correctly on $x = -|t|$, where $s = t_0$.

APPENDIX D. MÄRZKE-WHEELER COORDINATES FOR THE PARADOX OF
THE TWINS: CIRCULAR MOTION

In this scenario, we make the twins start together at the event \mathcal{F} with Lorentz coordinates $t = 0$, $x = R$, and $y = 0$. While the stationary twin Penelope stands fixed in space, Ulysses completes one circular orbit according to Eqs. (13) and (25), and rejoins Penelope at the event \mathcal{G} , defined by $t = 2\pi\Omega^{-1}\sqrt{1 + \Omega^2 R^2}$, $x = R$, and $y = 0$. After one revolution, Ulysses' proper time lapse is $\Delta\tau = 2\pi\Omega^{-1}$; Penelope's proper time coincides with the Lorentz coordinate time, so that her proper time lapse is $\sqrt{1 + \Omega^2 R^2}$ times Ulysses'. It turns out that this coefficient is just $\gamma = (1 - v^2)^{-1/2}$, because Ulysses moves with a constant velocity $v = \Omega R / \sqrt{1 + \Omega^2 R^2}$. In the end, we get the same differential aging of the twins as in the simpler linear geometry of App. C, and as predicted by a naïve application of the time dilation rule.

To study the local distribution of this differential aging, we need to determine the Märzke-Wheeler time (according to Ulysses) of all the events on Penelope's world-line. It is expedient to work in Lorentz polar coordinates centered around Penelope's location. Then Ulysses' world-line is given by

$$(38) \quad \begin{cases} t = \sqrt{1 + R^2\Omega^2} \tau, \\ \rho = 2R \sin \frac{\Omega\tau}{2}, \\ \theta = \frac{\pi}{2} - \frac{\Omega\tau}{2}. \end{cases} \quad (\text{Roto-Ulysses: world-line})$$

Let us now proceed in analogy with App. C. Eliminating the parameter τ , we describe Ulysses' world-line as

$$(39) \quad \mathcal{P}(t) : \rho = 2R \sin\left(\frac{\Omega t}{2\sqrt{1 + R^2\Omega^2}}\right). \quad (\text{Roto-Ulysses: world-line})$$

If we take only target events \mathcal{Q} on Penelope's world-line, the light-cone conditions (33) can be restated simply as

$$(40) \quad \begin{cases} \rho[\mathcal{P}(t_0 - s)] = t[\mathcal{Q}] - t[\mathcal{P}(t_0 - s)], \\ \rho[\mathcal{P}(t_0 + s)] = t[\mathcal{P}(t_0 + s)] - t[\mathcal{Q}], \end{cases}$$

where t_0 identifies an event along Ulysses' world-line, and t and s identify the simultaneous event (in the Märzke-Wheeler sense) along Penelope's world-line. Now, set $t = t[\mathcal{Q}]$ and use Eq. (39):

$$(41) \quad \begin{cases} 2R \sin\left(\frac{\Omega(t_0 - s)}{2\sqrt{1 + \Omega^2 R^2}}\right) = t - t_0 + s, \\ 2R \sin\left(\frac{\Omega(t_0 + s)}{2\sqrt{1 + \Omega^2 R^2}}\right) = t_0 + s - t. \end{cases}$$

We sum and subtract these two equations, and rearrange their terms:

$$(42) \quad \begin{cases} t = t_0 - 2R \sin\left(\frac{\Omega s}{2\sqrt{1 + \Omega^2 R^2}}\right) \cos\left(\frac{\Omega t_0}{2\sqrt{1 + \Omega^2 R^2}}\right), \\ s = 2R \sin\left(\frac{\Omega t_0}{2\sqrt{1 + \Omega^2 R^2}}\right) \cos\left(\frac{\Omega s}{2\sqrt{1 + \Omega^2 R^2}}\right). \end{cases}$$

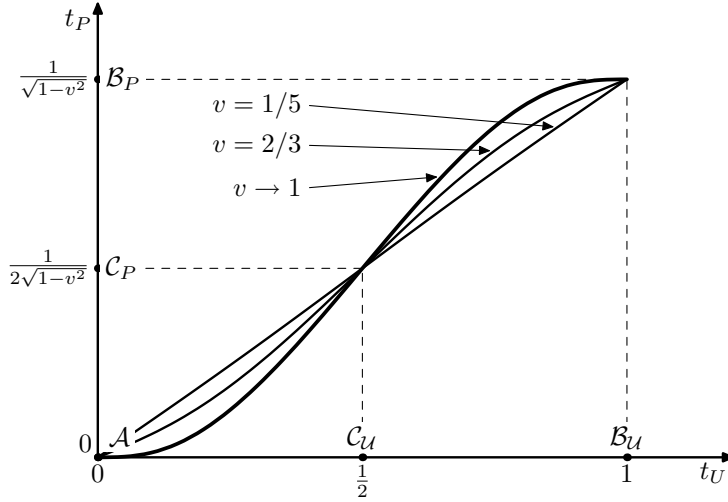


FIGURE 8: Circular version of the paradox of the twins. The graph shows Penelope's proper-time, in units of Ulysses' total proper-time lapse, as determined by Ulysses through Märzke-Wheeler slicing. In these renormalized units, the shape of the curve depends only on Ulysses' velocity. For $v \rightarrow 0$, the curve tends to a straight line; for $v \rightarrow 1$, to a limit curve.

These new equations must be solved together for t and s as functions of t_0 . The resulting distribution for differential aging is shown in Fig. 8, and it is a smoother version of the distribution that we obtained for the linear geometry of App. C (see Fig. 5). Interestingly, if we set

$$(43) \quad \{\tilde{t}, \tilde{s}, \tilde{t}_0\} = \frac{\Omega}{\sqrt{1 + \Omega^2 R^2}} \{t, s, t_0\},$$

and multiply Eqs. (42) by $\Omega/\sqrt{1 + \Omega^2 R^2}$, we find that the solutions $\tilde{t}(\tilde{t}_0)$ and $\tilde{s}(\tilde{t}_0)$ depend on the product ΩR , but not on Ω and R separately. This means that in these units, where the total elapsed Lorentz time is just 2π , the shape of curve that describes the aging distribution depends on Ulysses' absolute velocity ($\Omega R = v/\sqrt{1 - v^2}$), but not on the radius and angular frequency of his helix.

REFERENCES

- [1] C. W. Misner, K. S. Thorne, and J. A. Wheeler, *Gravitation*, Freeman, San Francisco, 1973.
- [2] C. Itzykson and J.-B. Zuber, *Quantum field theory*, McGraw-Hill, Singapore, 1985.
- [3] M. Pauri and M. Vallisneri, *Classical roots of the Unruh and Hawking effects*, Found. Phys. **29** (1999), 1499.
- [4] W. G. Unruh, *Notes on black hole evaporation*, Phys. Rev. D **14** (1976), 870.
- [5] R. F. Märzke and J. A. Wheeler, *Gravitation as geometry – I: the geometry of space-time and the geometrodynamical standard meter*, Gravitation and relativity (H.-Y. Chiu and W. F. Hoffmann, eds.), W. A. Benjamin, New York–Amsterdam, 1964, p. 40.
- [6] L. Page, *A new relativity. I. Fundamental principles and transformations between accelerated systems*, Phys. Rev. **49** (1936), 254.
- [7] H. E. Ives, *Extrapolation from the Michelson-Morley experiment*, J. Opt. Soc. Am. **40** (1950), 185.

- [8] G. J. Whitrow, *The natural philosophy of time*, Nelson, London and Edinburgh, 1961.
- [9] C. Kilmister and B. Tonkinson, *Pragmatic circles in relativistic time keeping*, Correspondence, invariance and heuristics: essays in honour of Heinz Post. (S. French and H. Kamminga, eds.), Kluwer, Dordrecht, 1993, p. 207.
- [10] R. M. Wald, *General relativity*, University of Chicago Press, Chicago, 1984.
- [11] J. L. Synge, *Timelike helices in flat spacetime*, Proc. Royal Irish Acad. **65A** (1967), 27.
- [12] J. R. Letaw, *Stationary world lines and the vacuum excitation of noninertial detectors*, Phys. Rev. D **23** (1981), 1709.
- [13] J. R. Letaw and Pfautsch J. D., *The stationary coordinate systems in flat spacetime*, J. Math. Phys. **23** (1982), 425.
- [14] W. Rindler, *Kruskal space and the uniformly accelerated frame*, Am. J. Phys. **34** (1975), 1174–1178.
- [15] A. Einstein, Ann. Phys. (Leipzig) **17** (1905), 891.
- [16] H. Arzelès, *Relativistic kinematics*, Pergamon Press, Oxford, 1966.
- [17] L. Marder, *Time and the space-traveller*, Allen and Unwin, London, 1971.
- [18] W. C. Salmon, *Space, time and motion: a philosophical introduction*, Dickenson, Encino, 1975.
- [19] M. Stautberg Greenwood, *Use of Doppler-shifted light beams to measure time during acceleration*, Am. J. Phys. **44** (1976), 259, Integration of the instantaneous received frequency from Doppler-shifted beacons is used to define simultaneity.
- [20] W. G. Unruh, *Parallax distance, time, and the twin “paradox”*, Am. J. Phys. **49** (1981), 589.
- [21] T. A. Debs and M. L. G. Redhead, *The twin “paradox” and the conventionality of simultaneity*, Am. J. Phys. **64** (1996), 384.
- [22] M. L. G. Redhead, *The conventionality of simultaneity*, Philosophical problems of internal and external worlds: essays on the philosophy of Adolf Grünbaum (J. Earman, A. I. Janis, G. I. Massey, and N. Rescher, eds.), Univ. of Pittsburgh, Pittsburgh, 1993, p. 103.